<Electronic Supplementary Information>

A water-stable multi-responsive luminescent Zn-MOF sensor for detecting TNP, NZF and $Cr_2O_7^{2-}$ in aqueous media

Xiaohe Wang,[a] Mingyuan Lei,[a] Tianjun Zhang,[a] Qingfu Zhang,[*a] Rufen Zhang,[a] and Ming Yang[b]

[a] *College of Chemistry and Chemical Engineering, Liaocheng University, Liaocheng 252059, China.*

[b] *Fujian Institute of Research on the Structure of Matter, Chinese Academy of Sciences, Fuzhou 350002, China*

X-ray crystallography

Single-crystal X-ray diffraction data were collected on a Bruker SMART-1000 CCD diffractometer with graphite-monochromated Mo Kα (λ = 0.71073 Å) radiation at room temperature. The structure was solved by direct methods and refined by the full-matrix least-squares methods on F^2 using the SHELX-97 program.[1] All non-hydrogen atoms were refined with anisotropic displacement parameters. The hydrogen atoms on amide groups were found from the different Fourier maps. Crystal and refinement data are summarized in Table S1, and selected bond lengths and bond angles are summarized in Table S2.

Table S1. Crystal data and structure refinement parameters for **1**.

Empirical formula	$C_{35}H_{28}N_4O_7Zn$
Formula weight	681.98
Temperature (K)	298(2)
Wavelength (Å)	0.71073
Crystal system	Monoclinic
Space group	$P2_1/c$
a (Å)	9.3019(7)
b (Å)	11.1262(8)
c (Å)	30.687(2)
β (°)	94.077(1)
Volume (Å^3)	3167.9(4)
Z	4

Calculated density (mg·m^{-3})	1.430
Absorption coefficient (mm^{-1})	0.832
F(000)	1408
Crystal size (mm)	0.31 × 0.20 × 0.07
Theta range for data collection (º)	2.647 to 25.019
Limiting indices	$-11 \leq h \leq 11$, $-11 \leq k \leq 13$, $-35 \leq l \leq 36$
Reflections collected/unique	15711/5567[R_{int} = 0.067]
Completeness to θ = 25.02º	99.6 %
Data/restraints/parameters	5567/0/426
Goodness-of-fit on F^2	1.077
Final R indices [$I>2\sigma(I)$]	R_1 = 0.058, wR_2 = 0.137

Table S2. Selected bond lengths (Å) and angles (°) for **1**.

Bond lengths			
Zn1-O1	1.977(3)	Zn1-O2B	1.984(3)
Zn1-O6A	1.968(4)	Zn1-N3	2.058(4)
Bond angles			
O1-Zn1-O2B	107.88(15)	O1-Zn1-O6A	111.92(15)
O1-Zn1-N3	108.89(16)	O2B-Zn1-O6A	122.30(15)
O2B-Zn1-N3	102.58(16)	O6A-Zn1-N3	102.06(18)

Symmetry codes, A: x+1, -y+1/2, z+1/2; B: -x+2, -y+2, -z+2.

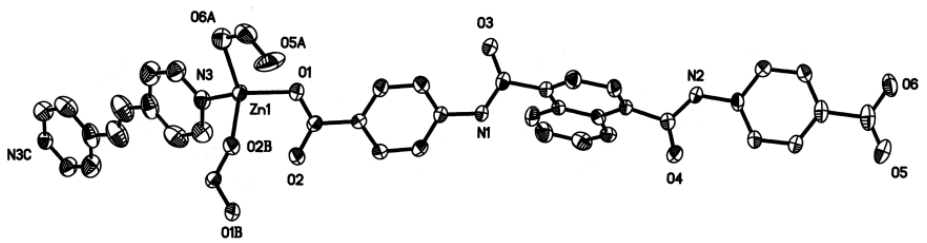

Fig. S1. A view of the asymmetric unit of **1** and the local coordination of the Zn(II) cation, the isolated DMF molecule and H atoms are omitted for clarity. Displacement ellipsoids are drawn at the 30% probability level. (Symmetry codes, A: x+1, -y+1/2, z+1/2; B: -x+2, -y+2, -z+2; C: -x+3, -y+3, -z+2).

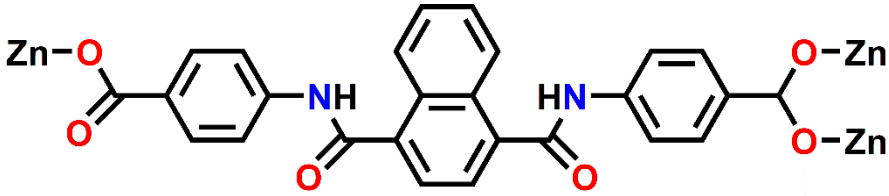

Fig. S2. Coordination mode of L^{2-} ligand in **1**.

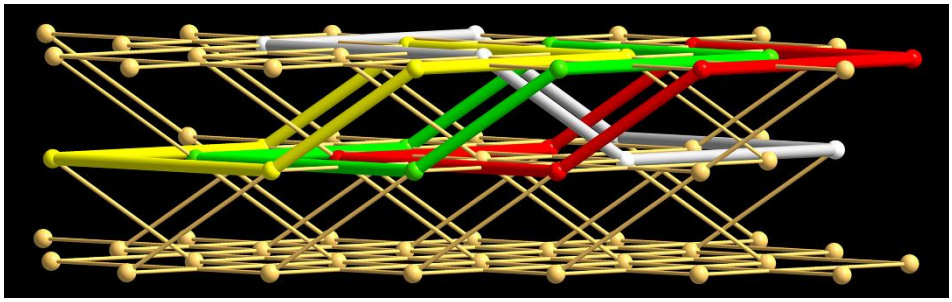

Fig. S3. Self-penetrating 6-connected network with $(4^4 \cdot 6^{10} \cdot 8)$ topology. The self-penetrating shortest circuits and rod are highlighted by red, green, yellow and white.

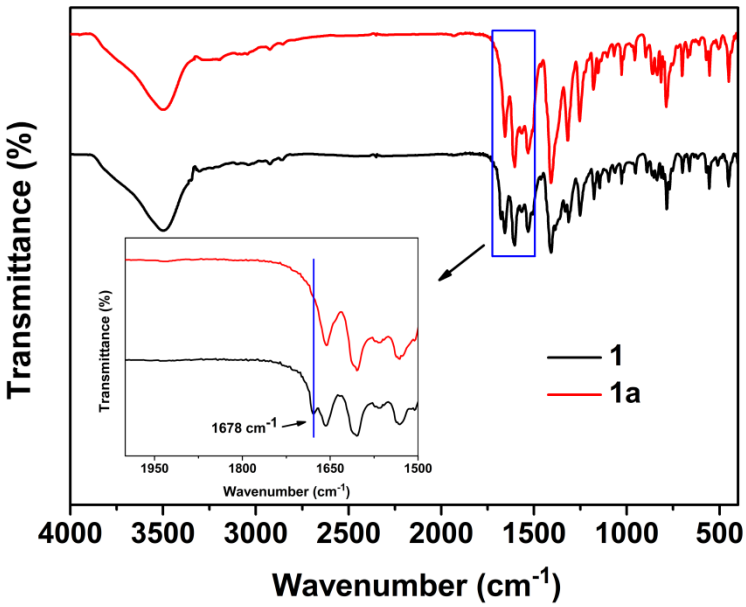

Fig. S4. The IR spectra for as-synthesized **1** and activated **1a** samples. Note that the C=O stretching vibration of the DMF was observed at 1678 cm^{-1} in the as-synthesized sample of **1**; this absorption peak disappeared in the activated sample of **1a**, indicating the complete removals of DMF after activation.

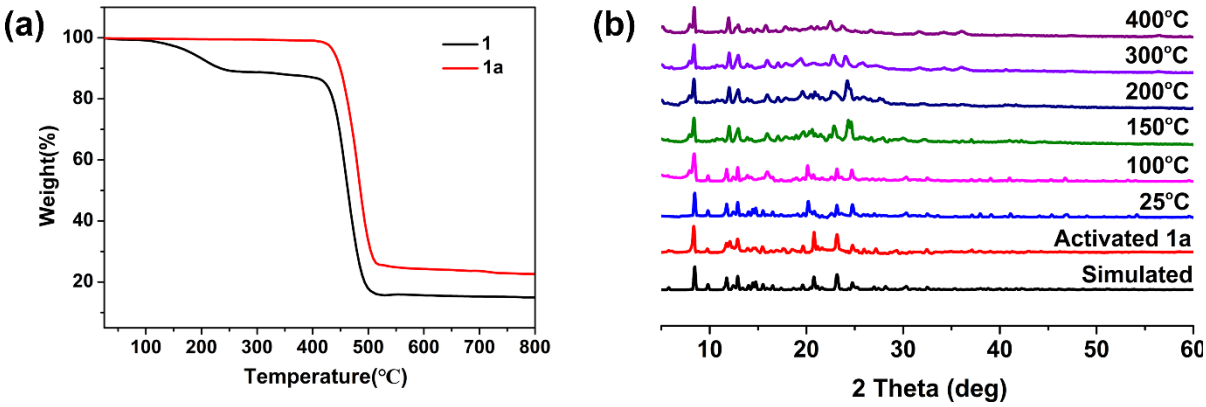

Fig. S5 (a) The TGA curve of **1** and **1a**. (b) The variable-temperature PXRD patterns for **1a**.

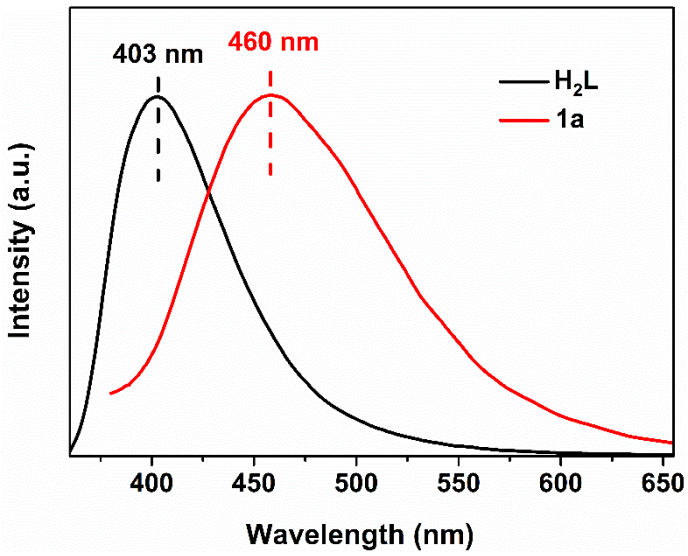

Fig. S6. The emission spectrum of H_2L ligand and complex **1a** dispersed in water at room temperature.

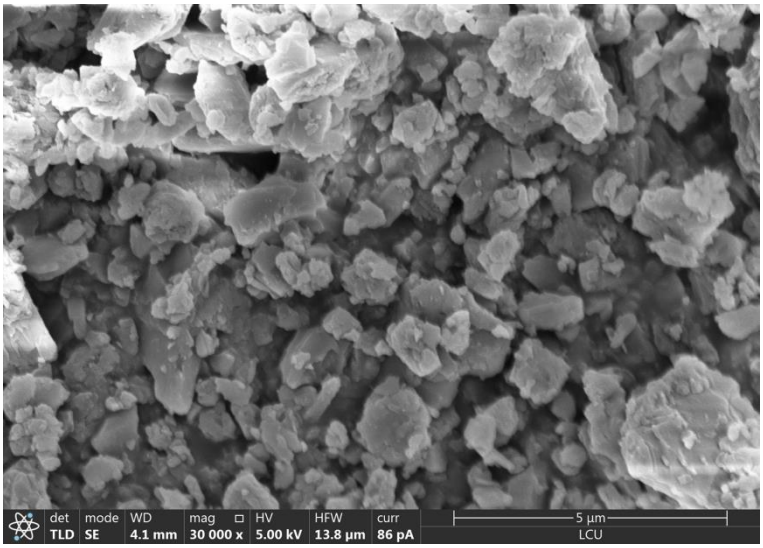

Fig. S7. The SEM of the ground samples for the sensing experiment.

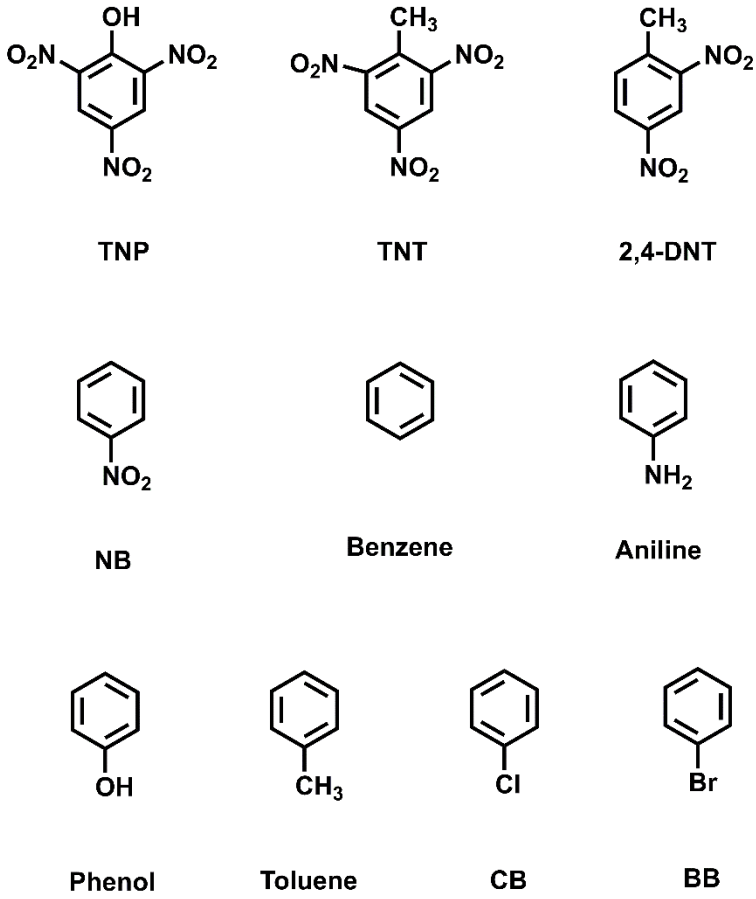

Fig. S8. Chemical structures of the investigated aromatic compounds.

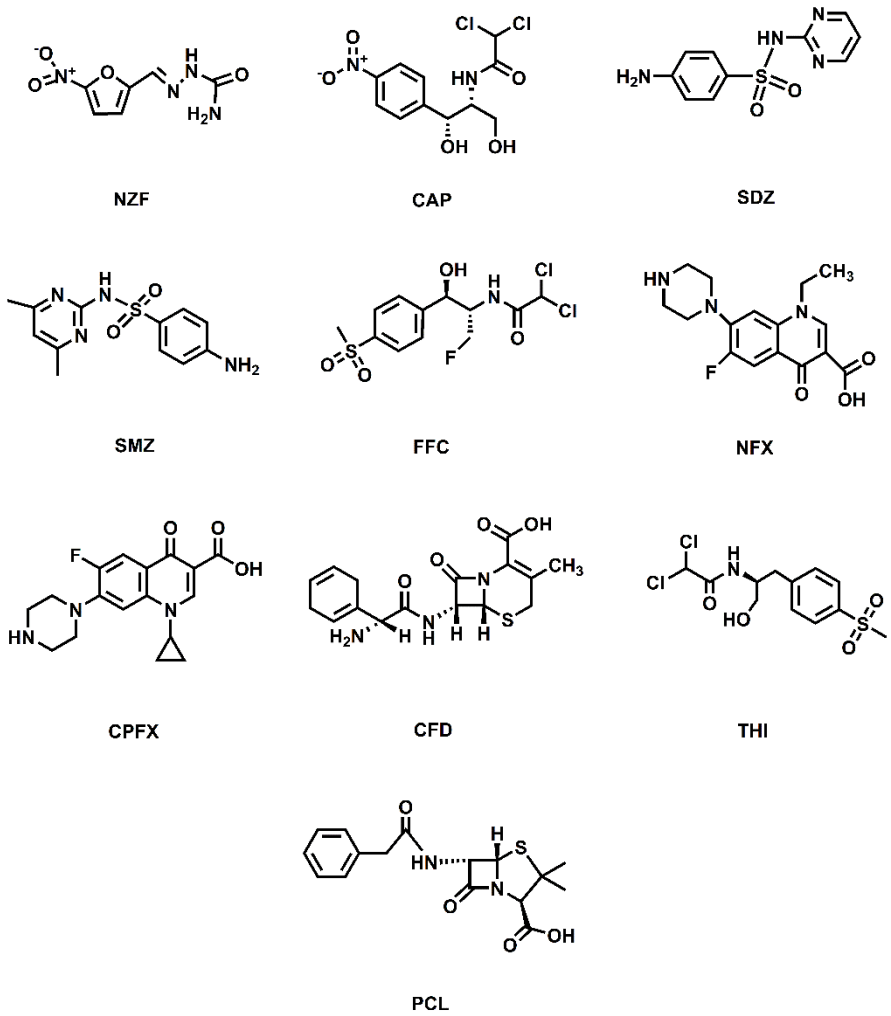

Fig. S9. Chemical structures of the investigated antibiotics.

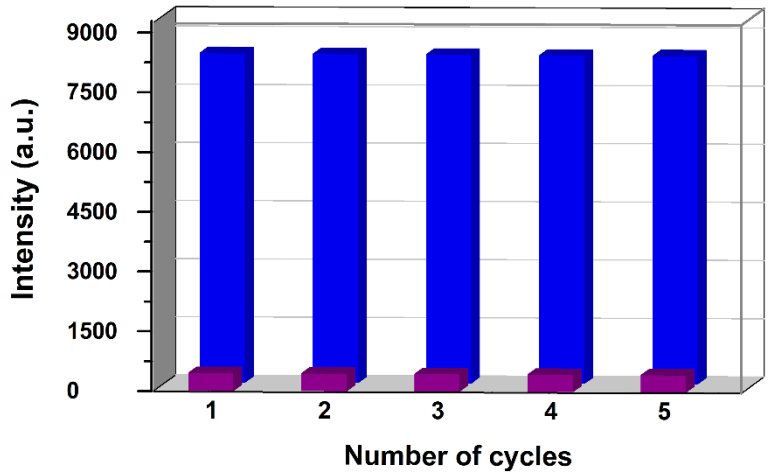

Fig. S10. Reversibility experiments of **1a** implemented with TNP.

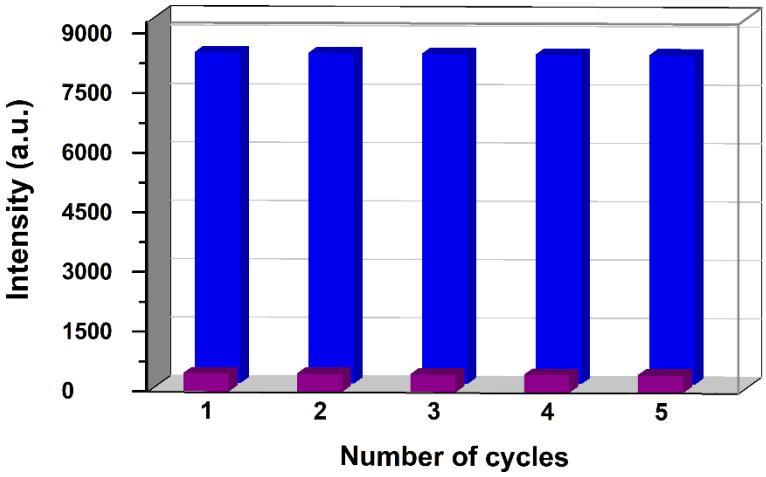

Fig. S11. Reversibility experiments of **1a** implemented with NZF.

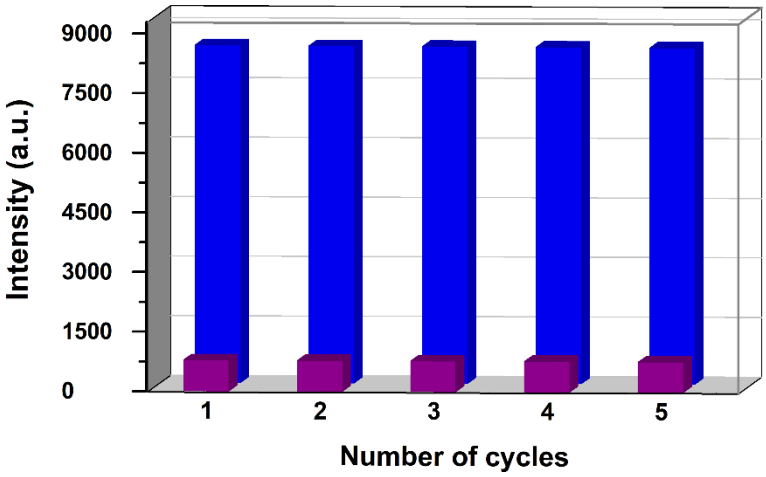

Fig. S12. Reversibility experiments of **1a** implemented with $Cr_2O_7^{2-}$ anions.

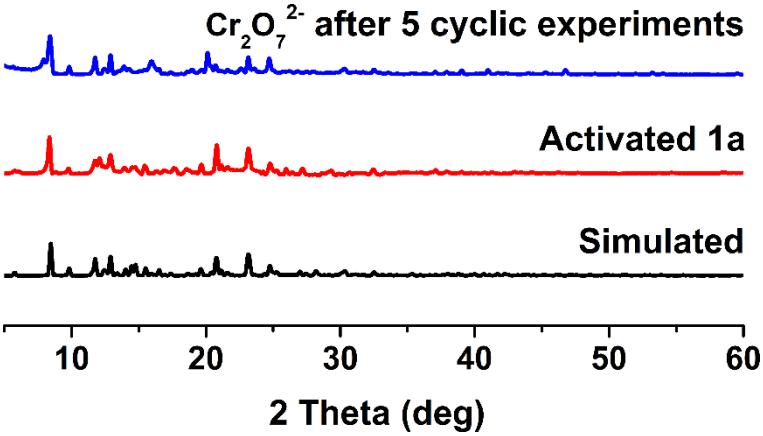

Fig. S13. The PXRD patterns for **1a** after 5 cyclic experiments.

Table S3. Comparison of the LOD in some reported TNP sensors.

MOFs	Analyte	LOD (ppb)	Ref.
$\{[W_2(\mu_3\text{-}S)_6(\mu_4\text{-}S)_2Cu_8(CN)_4(3\text{-abpt})]\cdot CH_3CN\cdot H_2O\}_n$	TNP	185.6	2
$[Zn(BPDPE)_2(dca)_2]_n$	TNP	167.2	3
$[NH_2(CH_3)_2][Zn_4O(bpt)_2(bdc\text{-}NH_2)_{0.5}]\cdot 5DMF$	TNP	128.3	4
UIO-66-Py	TNP	103.1	5
$\{[Zn(L)(bpe)_{0.5}]\cdot DMF\}_n$	TNP	61.5	This work

Table S4. Comparison of the LOD in some reported NZF sensors.

MOFs	Analyte	LOD (ppb)	Ref.
V102	NZF	200.0	6
$[Cd_2Na(L)(BDC)_{2.5}]\cdot 9H_2O$	NZF	162.0	7
Mg-APDA	NZF	108.0	8
$[Zn_4O(BCTPE)_3]$	NZF	100.0	9
$\{[Zn(L)(bpe)_{0.5}]\cdot DMF\}_n$	NZF	87.9	This work

Table S5. Comparison of the LOD in some reported $Cr_2O_7^{2-}$ sensors.

MOFs	Analyte	LOD (ppb)	Ref.
Tb-MOF-A	$Cr_2O_7^{2-}$	3909.4	10
NUM-5	$Cr_2O_7^{2-}$	700.0	11
NU-100	$Cr_2O_7^{2-}$	388.8	12
$\{[Zn(DCTP)]\cdot 4.2H_2O\}_n$	$Cr_2O_7^{2-}$	324.0	13
$\{[Zn(L)(bpe)_{0.5}]\cdot DMF\}_n$	$Cr_2O_7^{2-}$	59.2	This work

Table S6. HOMO and LUMO energies for the selected aromatic compounds and antibiotics calculated by density functional theory (DFT).

Analytes	HOMO (ev)	LUMO (ev)	Band Gap (ev)
TNP	-8.234	-3.896	4.338
TNT	-8.456	-3.491	4.965
2,4-DNT	-8.110	-2.975	5.135
NB	-7.589	-2.427	5.162
CB	-6.702	-0.342	6.360
benzene	-6.699	0.099	6.798
BB	-6.580	-0.343	6.237
phenol	-6.475	0.002	6.478
toluene	-6.402	0.145	6.547
aniline	-5.388	0.251	5.639
FFC	-6.620	-2.560	4.060
CAP	-6.579	-3.592	2.987
THI	-6.206	-2.661	3.545
NZF	-5.905	-3.724	2.181
PCL	-5.558	-1.777	3.781
SDZ	-5.538	-2.260	3.278
SMZ	-5.457	-1.898	3.559
CFD	-5.190	-1.990	3.200
CPFX	-4.850	-1.900	2.950
NFX	-4.700	-1.890	2.810

References

[1] G. M. Sheldrick, Acta Cryst., 2015, **C71**, 3-8.

[2] J. F. Zhang, Y. H. Liu, J. Y. Feng, L. P. Gong, M. G. Humphrey, C. Zhang, Inorg. Chem., 2019, **58**, 9749-9755.

[3] X. L. Zhang, J. S. Hu, B. Wang, Z. Q. Li, S. B. Xu, Y. N. Chen, X. M. Ma, J. Solid State Chem., 2019, **269**, 459-464.

[4] S. H. Xing, Q. M. Bing, H. Qi, J. Y. Liu, T. Y. Bai, G. H. Li, Z. Shi, S. H. Feng, R. R. Xu, ACS Appl. Mater. Interfaces, 2017, **9**, 23828-23835.

[5] Y. L. Tang, H. F. Wu, J. M. Chen, J. L. Jia, J. P. Yu, W. Xu, Y. Y. Fu, Q. G. He, H. M. Cao, J. G. Cheng, Dyes and Pigments., 2019, **167**, 10-15.

[6] S. L. Hou, J. Dong, X. L. Jiang, Z. H. Jiao, C. M. Wang, B. Zhao, Anal. Chem., 2018, **90**, 1516-1519.

[7] D. Zhao, X. H. Liu, Y. Zhao, P. Wang, Y. Liu, M. Azam, S. I. Al-Resayes, Y. Lu,W. Y. Sun, J. Mater. Chem. A, 2017, **5**, 15797-15807.

[8] N. Xu, Q. H. Zhang, B. S. Hou, Q. Cheng, G. A. Zhang, Inorg. Chem., 2018, **57**, 13330-13340.

[9] X. G. Liu, C. L. Tao, H. Q. Yu, B. Chen, Z. Liu, G. P. Zhu, Z. J. Zhao, L. Shen, B. Z. Tang, J. Mater. Chem. C, 2018, **6**, 2983-2988.

[10] H. H. Yu, J. Q. Chi, Z. M. Su, X. Li, J. Sun, C. Zhou, X. L. Hu, Q. Liu, CrystEngComm, 2020, **22**, 3638-3643.

[11] Z. Q. Yao, G. Y. Li, J. Xu, T. L. Hu, X. H. Bu, Chem.- Eur. J., 2018, **24**, 3192-3198.

[12] Z. J. Lin, H. Q. Zheng, H. Y. Zheng, L. P. Lin, Q. Xin, R. Cao, Inorg. Chem., 2017, **56**, 14178-14188.

[13] Y. Shi, T. Q. Song, C. S. Cao, B. Zhao, CrystEngComm, 2018, **20**, 6040-6045.